LAWRENCE
LIVERMORE
NATIONAL
LABORATORY

LLNL-JRNL-601472

Formulation of an RP-1 Pyrolysis Surrogate from Shock Tube Measurements of Fuel and Ethylene Time Histories

M. E. MacDonald, D. F. Davidson, R. K. Hanson, W. J. Pitz, M. Mehl, C. K. Westbrook

November 13, 2012

Fuel

Disclaimer

Formulation of an RP-1 Pyrolysis Surrogate from Shock Tube Measurements of Fuel and Ethylene Time Histories

Megan E. MacDonald, David F. Davidson, Ronald K. Hanson
Stanford University, Stanford, CA, 94305
William J. Pitz, Marcos Mehl, and Charles K. Westbrook
Lawrence Livermore National Laboratory, Livermore, CA 94550

RP-1 and ethylene time histories have been measured during RP-1 pyrolysis, allowing determination of ethylene yields and overall fuel decomposition rates for RP-1 near 20 atm and between 1050 K and 1500 K. A decomposition surrogate for RP-1 was formulated using the components n-dodecane, methylcyclohexane, and iso-cetane by targeting three decomposition characteristics of the fuel: compound class, overall fuel decomposition rate, and ethylene yield. Decomposition of this surrogate mixture was modeled using a newly developed detailed mechanism and the simulations are compared to the experimentally measured RP-1 and ethylene time histories. Comparisons between modeled and measured ethylene yields and overall fuel decomposition rates are also reported.

Nomenclature

a, b, c	=	mole fractions of dodecane, MCH, and iso-cetane, respectively, in a multi-component surrogate
I	=	laser intensity after passing through an absorbing medium
I_o	=	laser intensity before passing through an absorbing medium
L	=	path length through the absorbing medium in m
N	=	the number density (of fuel molecules) in the test mixture in mol/m^3
T	=	temperature in K
t	=	time
X	=	mole fraction
α	=	absorbance $\equiv -\ln(I/I_o)$
$\sigma(T, \lambda)$	=	absorption cross section (function of temperature and wavelength) in m^2/mol

1. Introduction

Interest in the decomposition chemistry of kerosene fuels has increased greatly in recent years. These fuels are often used for cooling rocket and high speed aircraft engines, and as the desire for greater engine efficiency and faster vehicles increases, the study of coke formation in the cooling system demands greater attention. To understand this coke formation process with intentions to mitigate or eliminate coke, one must begin with the vital initial step, fuel decomposition. It is important to know not only how quickly a fuel breaks apart, but also what decomposition products are formed during this process. Once these kinetic parameters have been determined for a fuel, a suitable surrogate mixture can be formulated to mimic these parameters.

Surrogates have long been a method for assisting in the study of a complex multi-component fuel by acting as a similar, but simpler, fuel. In many instances, conclusions formed based on the study of a surrogate can be extended to the fuel itself. They also provide modelers (in both kinetics and computational fluid dynamics) with a method of representing, during simulation, a fuel that may have hundreds of components. Computing the conditions for a reacting flow or running a kinetic simulation for the oxidation or pyrolysis of every component of a distilled fuel is beyond the current state-of-the-art. There is historical precedence for simulating the behavior of kerosene-type fuels with surrogates. A great number of surrogates exist in the literature which target the oxidation characteristics of kerosenes such as JP-8 and Jet-A [1-23], however, few have been proposed to simulate the behavior of RP-1. Those that exist are given in Tables 1-3.

From 1995 to 1997, Farmer et al. studied RP-1 and proposed two different multi-component surrogates that targeted compound class [24, 25]. These surrogates are given in Tables 1 and 2.

Table 1 First multi-component surrogate proposed by Farmer et al. [24]

Formula	Species	Mol %
$C_{13}H_{12}$	methylbiphenyl	17.4
$C_{12}H_{24}$	n-heptylcyclopentane	45.4
$C_{12}H_{28}$	n-tridecane	37.2

Table 2 Second multi-component surrogate proposed by Farmer et al. [25]

Species	Type	Formula	Vol %	Mole Fr
n-Undecane	Paraffin	$C_{11}H_{24}$	4.70	0.05013
Dodecane	Paraffin	$C_{12}H_{26}$	6.00	0.05948
n-Tridecane	Paraffin	$C_{13}H_{28}$	18.80	0.17828
n-Tetradecane	Paraffin	$C_{14}H_{30}$	12.50	0.10235
n-Hexylcyclopentane	Monocyclic Paraffin	$C_{11}H_{22}$	2.70	0.02921
n-Heptylcyclopentane	Monocyclic Paraffin	$C_{12}H_{24}$	3.60	0.03570
n-Octylcyclopentane	Monocyclic Paraffin	$C_{13}H_{26}$	11.20	0.10437
n-Nonylcyclopentane	Monocyclic Paraffin	$C_{14}H_{28}$	7.50	0.06547
Bicycloparaffin1	Polycyclic Paraffin	$C_{11}H_{20}$	11.30	0.13496
Bicycloparaffin2	Polycyclic Paraffin	$C_{12}H_{22}$	14.70	0.15453
Pentamethylbenzene	Mononuclear Aromatic	$C_{11}H_{16}$	1.30	0.01509
Hexamethylbenzene	Mononuclear Aromatic	$C_{12}H_{18}$	1.70	0.01758
Dimethylnaphthalene	Dinuclear Aromatic	$C_{12}H_{12}$	4.00	0.05285

More recently, the National Institute of Standards and Technology (NIST) has developed thermophysical surrogates for both RP-1 and RP-2, targeting physical and thermodynamic properties. These surrogates have been included in the NIST program REFPROP, which employs them to predict the thermophysical properties of RP-1 and RP-2 [26]. The NIST surrogates are listed in Table 3.

Table 3 Multi-component surrogates for RP-1 and RP-2 from Huber et al. [26]

	Composition, mole fraction	
Fluid	RP-1 surrogate	RP-2 surrogate
α-methyldecalin	0.354	0.354
5-methylnonane	0.150	0.084
2,4-dimethylnonane	0.000	0.071
n-dodecane	0.183	0.158
heptylcyclohexane	0.313	0.333

Although very few surrogates were found for RP-fuels, it is clear that extensive work has been published on oxidation surrogates for kerosene jet fuels. As with RP-1, however, the decomposition behavior of these kerosene fuels has not been as thoroughly studied as the oxidation behavior; very few decomposition surrogates were found for these fuels [9, 13]. Despite all that it offers to both experimentalist and computationalist, a surrogate is quite limited in the number of real-fuel properties that it can match. The user must be aware of the surrogate's intended purpose in order to utilize it correctly. Since a fuel surrogate is a simple representation of the actual fuel, it is not reasonable to expect that one surrogate can accurately simulate every aspect of the fuel. The extensive list of kerosene oxidation surrogates which were selected based on varying targets indicates a surrogate's dependence on the targeted characteristics. It is for this reason that the surrogate proposed here specifically targets the decomposition characteristics of RP-1. This study was carried out near 20 atm and between 1050 and 1500 K.

2. Theory

Time-histories and decomposition rates from shock tube/laser absorption experiments were obtained using Beer's law, Eq. (1), and the assumption of pseudo-first-order reactions. This process is described in further detail in references [27] and [28].

$$(I/I_o)_\lambda = \exp(-\sigma_\lambda N L) \quad (1)$$

The absorption cross section, σ_λ, of gaseous RP-1 was previously measured at 3.39 μm using both a Nicolet 6700 FTIR (for cross sections below 775 K) and a HeNe gas laser in a shock tube (for cross sections at temperatures above 800 K) [27].

In order to report ethylene yields, a knowledge of the cross section of ethylene is also necessary. The ethylene diagnostic utilizes both the 10.532 μm and 10.675 μm wavelengths of the CO_2 laser, and the ethylene cross sections for both wavelengths were reported in [28]. The two-wavelength interference correction method described in [28], together with the absorption cross sections for ethylene at these two wavelengths, can account for intermediate species that may interfere with the measurement of ethylene.

As discussed in [28], a major product of iso-alkane decomposition is iso-butene. Since a significant fraction of RP-1 is comprised of iso-alkanes (see Table 4), it would be reasonable to expect that iso-butene appears in the product mixture during RP-1 pyrolysis. MacDonald et al. also point out that the absorption cross section of iso-butene differs between the two CO_2 laser lines utilized for the ethylene diagnostic, prohibiting its direct subtraction out of the ethylene measurement [28]. However, the much larger difference in ethylene cross sections between the two lines, $\sigma_{C2H4,P14} - \sigma_{C2H4,P28} \approx 10\ (\sigma_{i\text{-}C4H8,P28} - \sigma_{i\text{-}C4H8,P14})$, means that any significant amount of ethylene will render the absorption of iso-butene at those wavelengths negligible. Modeling (see Section 6) indicates that the respective amounts of ethylene and iso-butene, $X_{C2H4} \approx 10\ X_{i\text{-}C4H8}$, are such that this is the case for all experiments here, except possibly for the lowest-temperature point (1051 K). For this shock experiment, the absorbance time histories at the P14 and P28 wavelengths are nearly equivalent, indicating that ethylene no longer dominates the absorbance. This low-temperature point was analyzed using the method developed for analysis of iso-cetane decomposition as described in reference [28], allowing for different cross sections of the interfering species at the two excitation wavelengths, while the ethylene mole fractions and ethylene yields for all other RP-1 shock experiments were calculated using the two-line ethylene diagnostic method described for analysis of dodecane and MCH decomposition in reference [28].

The absorption cross sections at 3.39 μm of all of the fuels considered here and their predominant pyrolysis products will be necessary for a comparison between the modeled and measured absorbance given in Section 6. Those for the fuels are given in references [27] and [28], while those for three primary product species have been measured in the current study and are shown in Fig. 1.

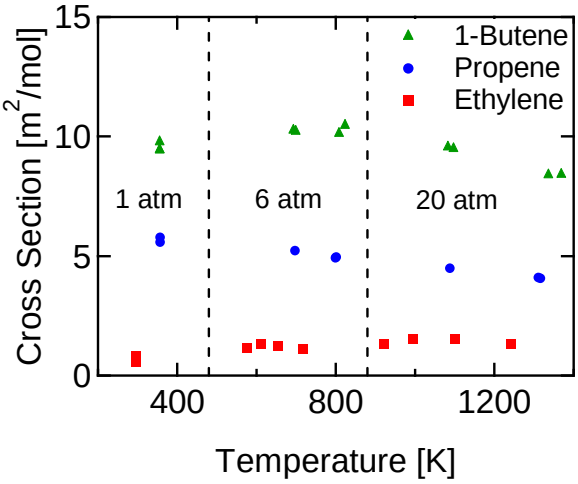

Fig. 1 Absorption cross sections of small alkenes at 3.39 µm.

3. Experimental Setup

The experimental setup employed in the current study is identical to that described by MacDonald et al. [28]. This setup is shown schematically in Fig. 2.

Two lasers were employed for these experiments. The Jodon HN-10GIR is a fixed-wavelength mid-infrared HeNe gas laser operating at 3.39 µm (2947.909 cm^{-1}), a wavelength that is strongly absorbed by all of the fuels studied. The Access Laser Company water-cooled LASY-4G CO_2 gas laser is operated at two different lines, P14 at 10.532 µm and P28 at 10.675 µm, which provide the diagnostic for the measurement of ethylene.

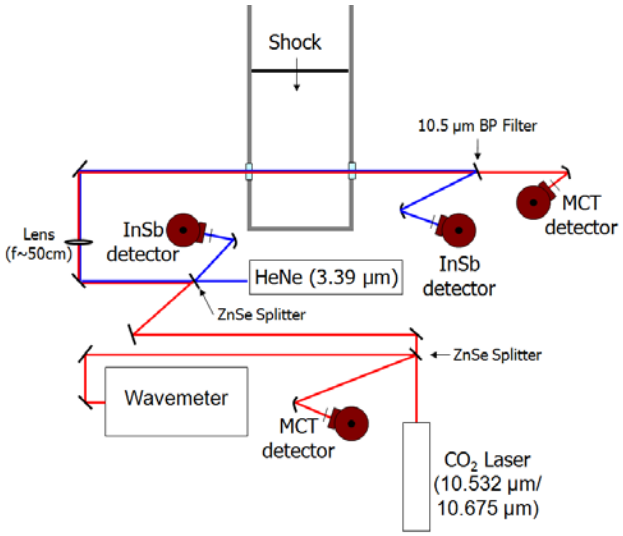

Fig. 2 Laser absorption experiment schematic.

Experiments were carried out in the heated High Pressure Shock Tube (HPST) facility at Stanford University. The high-pressure shock tube has a circular cross section, with an inner diameter of 5.0 cm and windows located 1.1 cm from the endwall. A detailed description of this shock tube was given by Petersen et al. [29, 30]. The HPST is heated in order to study low-vapor-pressure fuels, but when heating the mixing tank and shock tube, care must be taken to ensure that all of the components of RP-1 completely evaporate in the mixing tank and are transferred into the shock tube. This is confirmed with a simple experiment that is described in reference [27]. Figure 3 shows that complete evaporation occurs up to about 1 mL of RP-1 injected into the mixing tank.

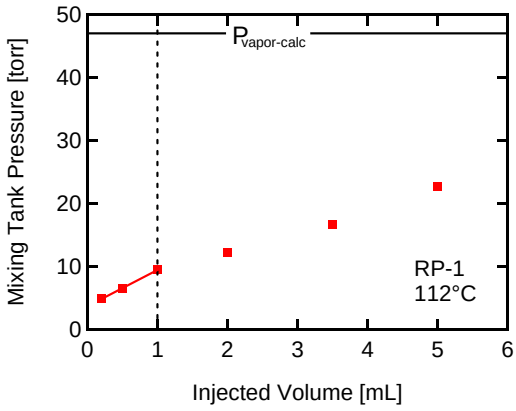

Fig. 3 HPST mixing tank complete evaporation check. Tank temperature 112°C, tank volume 12.84 L. Solid curve is a fit to the data. The beginning of the roll-off is indicated by the dashed line, and occurs at about 1 mL.

The roll-off seen in Fig. 3 is an indication that as additional RP-1 is injected, it no longer completely evaporates. Therefore, the maximum RP-1 volume injected into the mixing tank was 1.0 mL. Argon was then added up to the desired total pressure and the mixture was stirred in the tank. The RP-1 vapor was then transferred through heated lines into the shock tube at 83°C. The minimum detectable amount of fuel (with SNR of 1) at the conditions of this study is 50 ppm of RP-1. The fuel mole fraction was measured in the shock tube just prior to the shock using 3.39 μm laser absorption with the cross section calculated from the fits given in reference [27] and the measured temperature in region 1. The mole fraction calculated from the fuel and total pressures in the mixing tank was always within 13% of the absorption-measured mole fraction.

Because of the endothermic nature of pyrolysis, test gas mixture temperatures after the fuel decomposes will be slightly lower than the initial elevated temperatures immediately behind the reflected shock wave. Absorption cross-sections based on this lower temperature were used in the Beer's Law determination of C_2H_4 plateau yields from the absorption signals.

The RP-1 (lot number SH2421LS05) was obtained from the Air Force Research Laboratory (Edwards Air Force Base) and was refrigerated prior to use to avoid evaporation of the light components. RP-1 thermodynamic properties were determined from REFPROP [26, 31] and were used to formulate a seven-coefficient NASA polynomial [27]. This polynomial is a necessary input for the in-house code called FROSH that solves the normal shock jump equations and calculates the temperatures and pressures after both the incident and reflected shocks.

4. Results

Presented in Fig. 4 are the fuel and ethylene time histories during a sample RP-1 decomposition experiment. A more detailed explanation of how the fuel mole fraction was obtained from absorbance data is given in reference [27]. Figure 4b shows the peak ethylene yields during RP-1 decomposition. Ethylene yield is defined here as the plateau value of the ethylene mole fraction (or the peak value if the experiment is hot enough that once formed, the ethylene starts to decompose) divided by the initial fuel mole fraction. In other words, it is the number of ethylene molecules formed per initial fuel molecule. Assuming the RP-1 values for molecular weight (170 g/mol) and H/C ratio (2.1), an ethylene yield of 2 is equivalent to a conversion of carbon in the form of RP-1 to the form of ethylene of 33%.

It should be noted that the RP-1 mole fractions shown in Figs. 4 and 5 were determined by subtracting the long-time product absorbance from the total measured fuel and product absorbance. In some cases at later times when the product absorbance is significantly larger than the absorbance from RP-1, this subtraction resulted in noise-generated negative values for the RP-1 mole fraction.

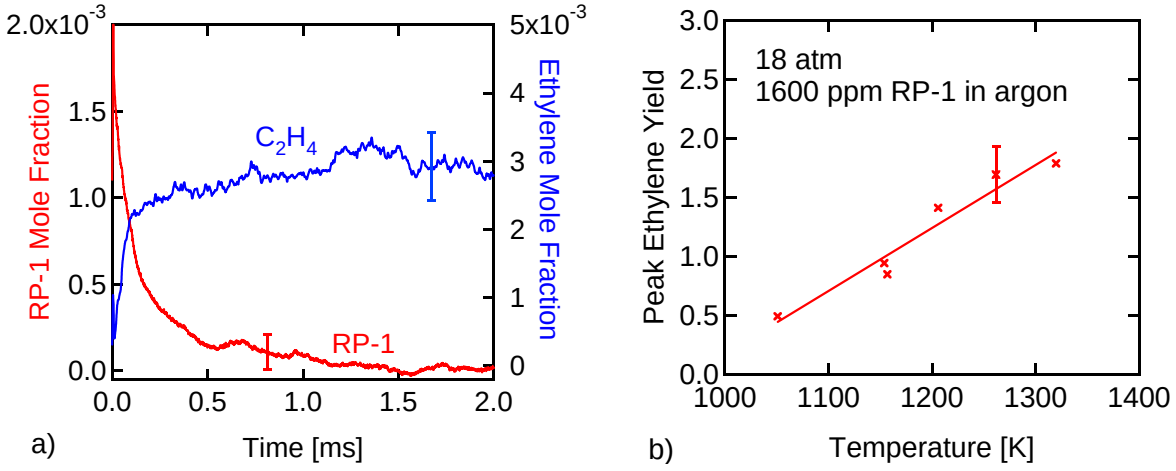

Fig. 4 RP-1 decomposition, a) initial reflected shock conditions: 1262 K, 18.4 atm, 0.17% RP-1 in argon, b) measured peak ethylene yields as a function of temperature.

Figure 5 shows the fuel and ethylene time histories for RP-1 decomposition shock experiments at five different temperatures. As expected, the higher the temperature, the faster RP-1 is removed. The lowest-temperature experiment resulted in a mixture that was not dominated by ethylene. Therefore, the method described by MacDonald et al. [28] was utilized to obtain long-time yield values for ethylene, propene, and iso-butene, but no time history is reported for this point. The uncertainties shown in Fig. 4 and listed in Fig. 5 are propagated uncertainties calculated using the method described in reference [27]. The major contributor to the uncertainty in the ethylene measurement was the uncertainty in the cross section of ethylene at 10.675 μm, the CO_2 laser's P28 line.

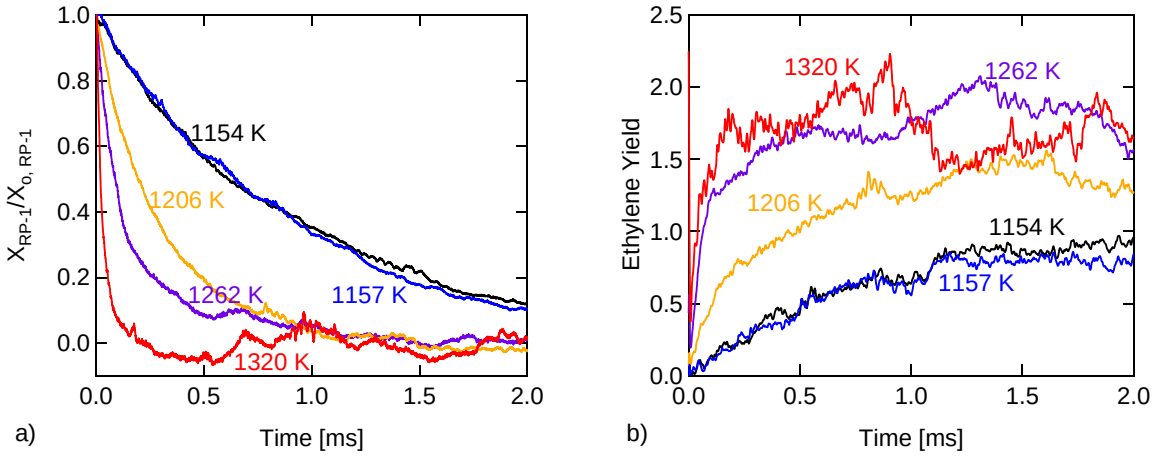

Fig. 5 RP-1 decomposition. Initial reflected shock conditions: 1051 - 1320 K, 18.4 – 20.4 atm, 0.14 – 0.17% fuel in argon. a) Normalized RP-1 mole fraction. b) Ethylene yields. Uncertainty (as shown Fig. 4) is ±100 ppm for RP-1 and ±500 ppm for ethylene.

5. Formulation of an RP-fuel Decomposition Surrogate

As mentioned in Sec. 1, very few RP-fuel surrogates have been proposed to date and those that do currently exist target only compound class or thermophysical properties. While a much more extensive list of jet-fuel (JP-8 and Jet-A) surrogates has been proposed [1-22], the variety of components utilized in the existing surrogates leads to the obvious conclusion that the selection of a surrogate depends greatly on the target. As of yet, no studies have targeted decomposition in their formulations of multi-component surrogates for RP-fuels.

Three characteristic traits of decomposition are targeted in this study: compound class, overall fuel decomposition rate, and ethylene yield. As checks to ensure that this surrogate represents RP-1 as closely as possible, the molecular weight and H/C ratio of the surrogate mixture will also be considered in the formulation process. First, compound class will be considered.

For the purpose of simplicity, many studies assume a single-component surrogate for chemical kinetic purposes, but in doing so, neglect the finite effects of various hydrocarbon compound classes on the kinetics of the real fuel. For example, while the decomposition of a branched alkane results in a mixture containing mostly ethylene and other small straight-chain alkenes and alkanes [32, 33], Holman et al. state clearly that during the pyrolysis of iso-cetane, iso-butene constituted 50% of the resulting species, making it by far the most predominant pyrolysis product [34]. This is in accord with the LLNL – iso-cetane predictions for all temperatures studied here, in which the most prevalent species resulting from iso-cetane decomposition is iso-butene, followed by propene, methane, and ethane. Both the LLNL - MCH [35] and JetSurF 2.0 [36] mechanisms predict ethylene as the primary product and propene as a less abundant, but still major, product. However, these mechanisms differ slightly in their prediction of the identities of other major products. LLNL - MCH predicts that 1,3-butadiene and methane are major constituents of the product mixture, while JetSurF 2.0 predicts 1-butene and acetylene. At the highest temperature studied here, near 1500 K, both mechanisms predict large amounts of acetylene and methane, and benzene also appears as a significant product. Since the decomposition all three of these compound classes result in quite different species mixtures, and since RP-fuels contain representatives from all three, it will be necessary to formulate a multi-component surrogate if this surrogate is to be useful in modeling the decomposition behavior of RP-fuels. A recent publication by

Billingsley et al. clearly indicates the breakdown of compound classes in RP-1 and RP-2 [37]. This is shown in Table 4.

Table 4 Average RP-1/RP-2 Class Composition [37]

Hydrocarbon Type	Mass %
Paraffins	
n-	5
iso-	39
Total	**44**
Cylcoparaffins	
Cycloparaffins	34
Dicycloparaffins	17
Tricycloparaffins	4
Total	**55**
Aromatics	
Alkylbenzenes	0.5
Indans+Tetralins	<0.5
Naphthalene	<0.5
Naphthalenes	0.5
Total	**1**

It is immediately apparent that a major fraction of RP-fuels are cycloparaffins (cycloalkanes). Several cycloalkanes are readily available, including methylcyclohexane (MCH), n-propylcyclohexane, and n-butylcyclohexane. Although any of these could serve as a representative of the cycloalkane group, MCH has commonly been used to represent cycloalkanes in many jet-fuel surrogates [3, 7, 10, 18-21] and previous studies of both its pyrolysis [38-44] and oxidation [19, 23, 35, 44-46] can be found in the literature. Thus MCH was selected as the cycloalkane for the proposed surrogate. Although it is important to capture the chemistry of each compound class contained in RP-fuels, including a two- or three-ringed cycloalkane would greatly increase the complexity of the surrogate. For this reason, and because single-ringed cycloalkanes represent the majority of the cyclocalkanes in Table 4, multi-ring cycloalkanes will be grouped into an all-inclusive cycloalkane group that will be represented by MCH.

Another notable aspect of Table 4 is the split between normal and branched alkanes. Many historically reported compound class breakdowns neglect to distinguish between normal and branched alkanes. This, and the difference in composition between RP-fuels and most jet fuels (which contain a larger percentage of n-alkanes [20]), explains why most jet-fuel surrogates utilize primarily normal alkanes. It is apparent from Table 4 that the majority of alkanes in RP-1 and RP-2 are actually branched. Albright et al. [47] and Frey et al. [48, 49] indicate that normal and branched alkanes containing an equivalent number of carbon atoms decompose at different rates. Also, Agosta et al. [23] emphasize the importance of including both normal and branched alkanes in a JP-8 surrogate intended to match kinetic targets. For these reasons, it will be important to include a both a normal and a branched alkane in the proposed surrogate.

As the two readily-available branched alkanes are iso-octane and iso-cetane, these were considered as the options in selecting a suitable branched alkane. N-dodecane will be utilized as the normal alkane due to the extensive decomposition work that already exists concerning this hydrocarbon [27, 28, 32, 33, 50-63], and also because it matches the H/C ratio of RP-1 quite closely.

By matching compound class, the RP-1 decomposition surrogate components have been narrowed to MCH, n-dodecane, and either iso-octane or iso-cetane. Having noted this, the second target, overall fuel decomposition rate, will be considered. Overall fuel decomposition rates for RP-1 were calculated from the measured RP-1 time history with the method described in reference [27] which assumes first-order decomposition kinetics and employs Beer's Law to produce both the fuel mole fraction time history and overall fuel decomposition rate. Figure 6 shows the recently-measured high-temperature overall fuel decomposition rates for RP-1. Also shown are similar rates for n-dodecane [27, 28], iso-octane [64], iso-cetane [28], and MCH [28].

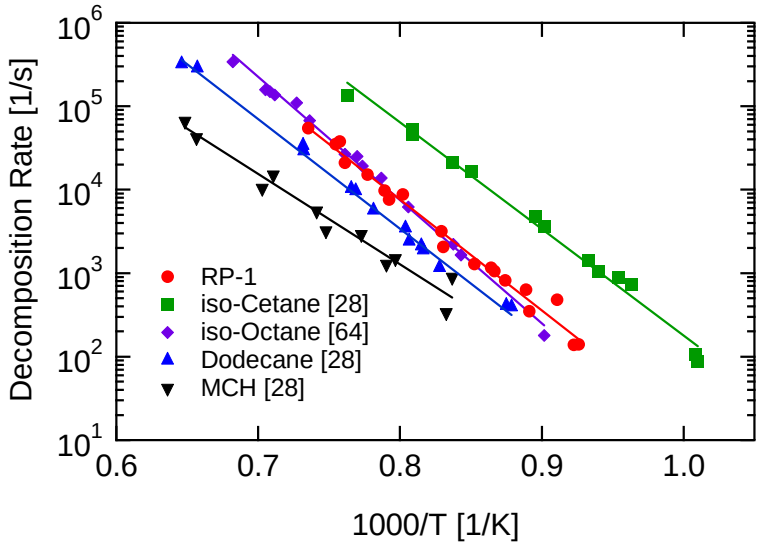

Fig. 6 Decomposition rates of RP-1 (18.4 to 20.4 atm, 0.14 to 0.17% fuel in argon) and possible surrogate components. Dodecane, iso-Cetane, and MCH data from [28], 15.3 to 22.2 atm, 0.11 to 0.2% fuel in argon. Iso-Octane data from [64], 1.6 to 2.0 atm, 0.01 to 0.05% fuel in argon.

It is apparent in Fig. 6 that n-dodecane decomposes more slowly than RP-1 and is thus not an ideal single-component decomposition surrogate. If the only target were decomposition rate, iso-octane would be the ideal surrogate. However, a single-component surrogate would not match the compound classes of RP-1 and would therefore poorly predict the product distribution resulting from its decomposition. Furthermore, iso-octane has a much lower molecular weight and a much higher H/C ratio than RP-1. Thus it becomes necessary to utilize a branched alkane that is both heavier and decomposes faster than iso-octane in order to balance out the effects of the slowly-decomposing n-dodecane. The observed trend for alkanes, both normal and branched, is that with increasing molecular weight, the overall fuel decomposition rate also increases. As seen in Fig. 6, iso-cetane indeed follows this expected trend and decomposes faster than iso-octane, making it the ideal third component in an RP-1 decomposition surrogate.

The third consideration in selecting a suitable RP-1 decomposition surrogate is ethylene yield. Ethylene is a primary product in the decomposition of dodecane, MCH, and RP-1 which makes it an ideal species to use as a target for the proposed RP-1 decomposition surrogate. Measurements of ethylene yield for dodecane, MCH, and iso-cetane were reported in reference [28]. Measured ethylene yields for RP-1 are given in Fig. 4 and the comparison of all measured yields is shown in Fig. 7. A cursory look at Figs. 6 and 7 shows that the decomposition rate of RP-1 can be matched with a combination of only MCH and iso-cetane. However, dodecane must be included in the mixture in order to match the RP-1 ethylene yield. This confirms the necessity of utilizing all three possible surrogate components studied in reference [28] for a multi-component RP-1 decomposition surrogate.

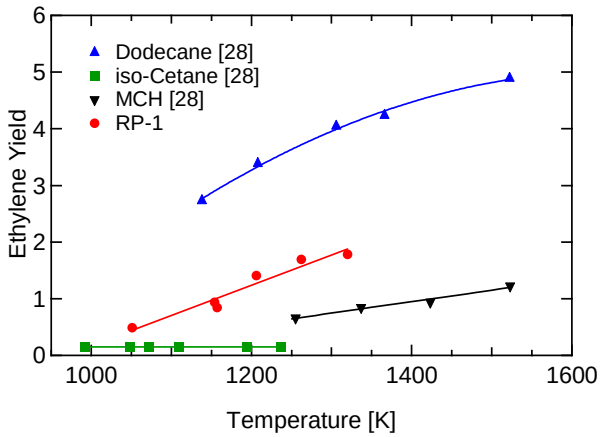

Fig. 7 Ethylene yields during decomposition of RP-1 and three possible surrogate components. Solid lines are best fits to the data. Dodecane, iso-Cetane, and MCH data from [28].

The compound class target has now been satisfied, and the overall fuel decomposition rate and ethylene yield targets have been useful in the process of identifying the necessary components. These last two targets will now be completely satisfied through the selection of the mole fractions of each surrogate component. Throughout the discussion of the next two targets, it will be assumed that both decomposition rate and ethylene yield are linearly additive when mixtures of fuels are considered. The accuracy of this assumption has been debated in the literature, as Albright, Cyril, and Corcoran [47] state that "In general, if two paraffins are cracked in admixture, they behave as if they were cracked separately. Both rates and selectivities are unchanged." Agosta et al. [23], however, maintain that "the autoignition properties of the mixture cannot be simply reproduced by linear blending rules." Although the latter statement was directed at the oxidation process, it is a warning that for kinetic purposes, linear blending rules may not result in a mixture with the expected behavior. However, as no other blending strategies have been proposed, linear blending rules will be utilized here to estimate an RP-1 pyrolysis surrogate. With this assumption, these two remaining targets can be satisfied in a straightforward manner. Listed in Table 5 are the best fit polynomials for the ethylene yields (Fig. 7) and overall fuel decomposition rates (Fig. 6) of all three surrogate components and for RP-1 itself.

Table 5 Best-fit polynomials for overall fuel decomposition rates and ethylene yields

Fuel	Decomposition Rate [1/s]	Ethylene Yield
n-dodecane	x = 1.06e14 exp(-30200/T)	p = -8.98e-6 T^2 + 2.97e-2 T – 19.3
MCH	y = 5.73e11 exp(-24900/T)	q = 2.15e-3 T – 2.00
iso-cetane	z = 1.05e15 exp(-29400/T)	r = 0.15
RP-1	k = 3.26e14 exp(-30600/T)	e = 5.68e-3 T + 5.49

Letting x, y, z, and k represent the overall fuel decomposition rates of dodecane, MCH, iso-cetane, and RP-1, respectively, the overall fuel decomposition rate target can be satisfied with the equation ax+by+cz = k, where a, b, and c are the mole fractions of dodecane, MCH, and iso-cetane, respectively. Similarly, letting p, q, r, and e be the ethylene yields for dodecane, MCH, iso-cetane, and RP-1, respectively, the ethylene yield target can be satisfied with the equation ap+bq+cr = e. Noting that this mixture must have mole fractions summing to one, the third equation necessary to solve this linear system is clearly a+b+c = 1. Apparent in Table 5 is the temperature dependence of each variable listed. This temperature dependence of the target variables means that the ideal surrogate composition will also vary with temperature, and this is shown in Fig. 8.

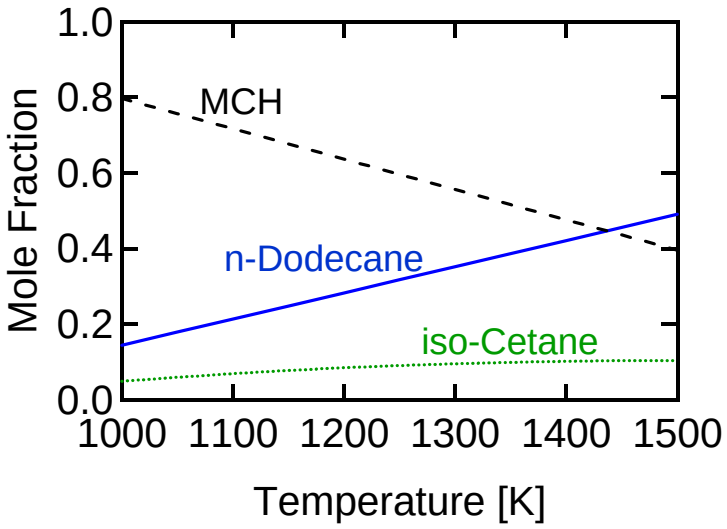

Fig. 8 Composition of an RP-1 decomposition surrogate as a function of temperature.

The mixture selected for comparison with measured RP-1 data was an average composition over the 1000 – 1500 K temperature range. This mixture is 32% dodecane, 59% MCH, and 9% iso-cetane. Its molecular weight is 133 g/mol, which is about 22% lower than that of RP-1 (170 g/mol), but its H/C ratio is 2.06, quite close to that of RP-1, which is given as 2.1 [65]. Its comparison with the RP-1 overall fuel decomposition rate is shown in Fig. 9 and with the measured RP-1 ethylene yields is shown in Fig. 10.

In Fig. 9, the best fits to the measured dodecane, MCH, and iso-cetane overall fuel decomposition rates are shown in order to provide a reference for how well the surrogate mixture matches the RP-1 data shown. The maximum difference between the RP-1 overall fuel decomposition rate data and those calculated for the surrogate mixture is 50%.

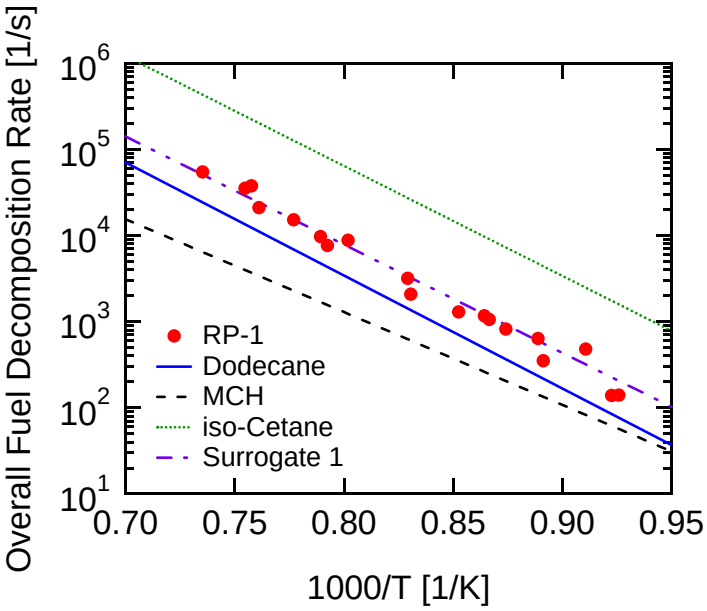

Fig. 9 Comparison of measured RP-1 overall fuel decomposition rates with the linear combination of the measured overall fuel decomposition rates from the surrogate components. Dodecane, iso-Cetane, and MCH data from [28].

Figure 10 shows a similar comparison for ethylene yield. Here it is apparent that this temperature-averaged surrogate matches the temperature-dependent surrogate near 1150 K. The slope of the ethylene yield curve for the surrogate is obviously dominated by its major component, MCH. The maximum difference between the RP-1 ethylene yield and those calculated for the surrogate mixture is 55% at the lowest temperature (difference in yield of 0.3).

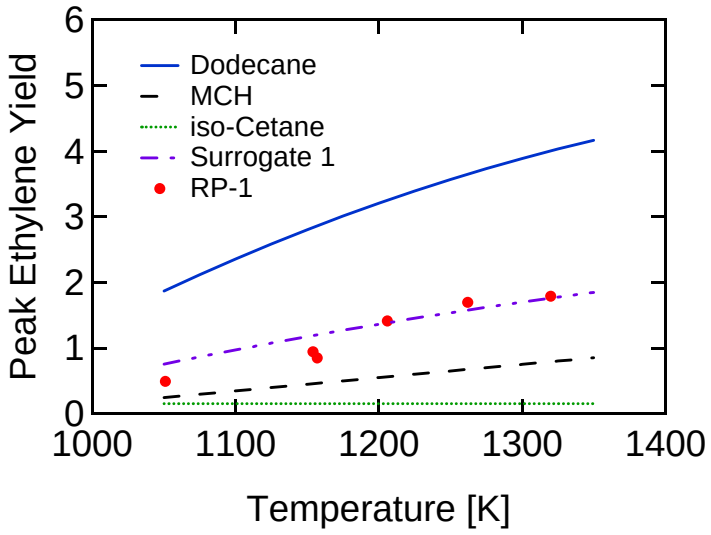

Fig. 10 Comparison of measured RP-1 ethylene yields with the linear combination of the measured overall ethylene yields from the surrogate components. Dodecane, iso-Cetane, and MCH data from [28].

6. Mechanism Predictions

Since this new RP-1 pyrolysis surrogate utilizes three species, each from a different compound class, it was necessary to combine the existing mechanisms for each component into a new all-inclusive mechanism. This was carried out with the LLNL – n-alkane [66], MCH [35], and iso-cetane [67] mechanisms and the resulting mechanism will be referred to as LLNL – mix. It has been utilized here along with the newly-proposed surrogate to simulate the decomposition behavior of RP-1.

Figure 11 shows the absorbance time history for the 3.39 μm HeNe laser. At early times, absorption at this wavelength is dominated by the fuel, while at later times, the absorbance plateau is due to absorption from the resulting decomposition product species. As measurement of the mole fractions of each of these resulting species would require more wavelengths than were utilized in this study, a comparison is made between the total measured absorbance at 3.39 μm and the model-predicted absorbance at 3.39 μm. This predicted absorbance time history was modeled using the LLNL – mix mole fractions for dodecane, MCH, iso-cetane, ethylene, propene, and iso-butene and the cross sections of each which are given in references [27] and [28] and Section 2. Based on the low-temperature and low-pressure cross section data from reference [68] for iso-butene in the 3.4 μm region, the cross section of iso-butene at 3.39 μm and the conditions of interest was estimated to be 10 m^2/mol. Figure 11 shows both the comparison of measured and modeled absorbance time histories for a sample shock experiment and the comparison between measured RP-1 overall fuel decomposition rates and rates predicted by the model composed of the selected surrogate and the LLNL-mix mechanism. Although the absorption characteristics of the surrogate components were not considered in the selection of this mixture, the initial predicted absorbance in Fig. 11a is only about 10% lower than the initial measured absorbance. Throughout the rest of the absorbance time history, the predicted absorbance matches the measured absorbance to within 30%. For these RP-1 experiments, the maximum difference between the predicted absorbance and the measured absorbance was on average 35%. Figure 11b shows the comparison between measured and modeled overall fuel decomposition rates. It is clear from this figure that the chosen surrogate matches the overall fuel decomposition rate of the actual fuel best near the temperature at which the mixture was selected (see Fig. 8).

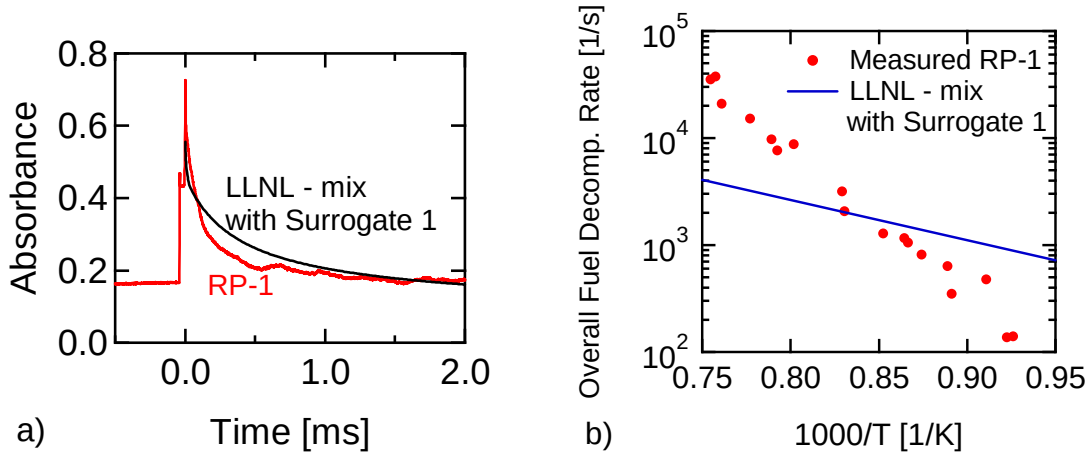

Fig. 11 Comparison of measured and predicted a) absorbance for initial reflected shock conditions: 3.39 µm. 1262 K, 18.4 atm, 0.17% RP-1 in argon. b) overall fuel decomposition rates, 18.4 to 20.4 atm, 0.14 to 0.17% fuel in argon.

The predicted ethylene time history during decomposition is shown in Fig. 12a as compared to that measured during RP-1 decomposition at 1262 K and ethylene yields for each RP-1 experiment with their corresponding modeled yields are shown in Figure 12b.

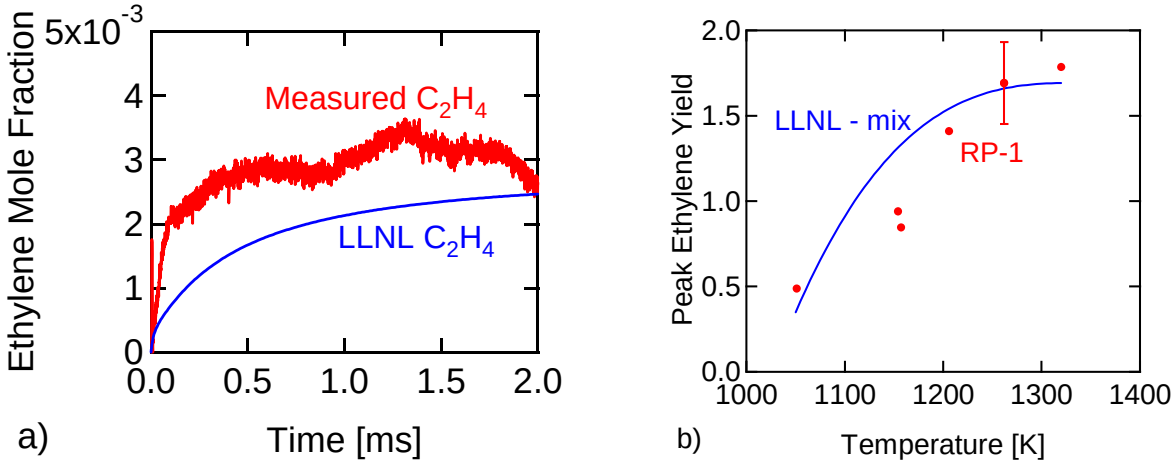

Fig. 12 Ethylene measurements during RP-1 decomposition. a) Comparison of measured and modeled ethylene time histories at initial reflected shock conditions: 1262 K, 18.4 atm, and 0.17% fuel in argon. b) Comparison of measured RP-1 and LLNL-mix + Surrogate 1-predicted ethylene yields. Modeled results utilized Surrogate 1 for RP-1.

The LLNL – mix mechanism and Surrogate 1 combination actually predict the measured RP-1 ethylene yield relatively well. It should be noted that both the mechanism and the surrogate were developed completely independently from the RP-1 measurements.

7. Conclusion

An RP-1 decomposition surrogate was formulated based on three targets: compound class, overall fuel decomposition rate, and ethylene yield. This surrogate contains 32% dodecane, 59% MCH, and 9% iso-cetane and captures the RP-1 overall fuel decomposition rate to within 50% and ethylene yield to within 55%. Comparison

with a newly-developed mechanism indicates that three predominant products of RP-1 decomposition are ethylene, propene, and iso-butene and that as temperature increases, the production of ethylene increases.

Acknowledgments

This work was supported by ERC Incorporated at the Air Force Research Laboratory, with Dr. David Campbell as program manager and Matthew Billingsley as contract monitor. Model development work by CKW, WJP and MM was performed under the auspices of the U.S. Department of Energy by Lawrence Livermore National Laboratory under Contract DE-AC52-07NA27344. These input files for the LLNL - mix model are available as Supplementary material to this publication and from the LLNL website at: https://www-pls.llnl.gov/?url=science_and_technology-chemistry-combustion.

References

[1] Catalanotti E, Hughes KJ, Pourkashanian M, Wilson CW. Development and application of a surrogate distillate fuel. Energy and Fuels 2011;25:1465–1473.

[2] Colket M, Edwards T, Williams S, Cernansky NP, Miller DL, Egolfopoulos F, Lindstedt P, Seshadri K, Dryer FL, Law CK, Friend D, Lenhert DB, Pitsch H, Sarofim A, Smooke M, Tsang W. Development of an experimental database and kinetic models for surrogate jet fuels. 45th AIAA Aerospace Sciences Meeting 2007; AIAA 2007-770.

[3] Cooke JA, Bellucci M, Smooke MD, Gomez A, Violi A, Faravelli T, Ranzi E. Computational and experimental study of JP-8, a surrogate, and its components in counterflow diffusion flames. Proc Comb Inst 2005;30:439–446.

[4] Dagaut P. On the kinetics of hydrocarbons oxidation from natural gas to kerosene and diesel fuel. Phys Chem Chem Phys 2002;4:2079–2094.

[5] Edwards T, Maurice LQ. Surrogate mixtures to represent complex aviation and rocket fuels. , J Prop Power 2001;17:461–466.

[6] Gokulakrishnan P, Gaines G, Currano J, Klassen MS, Roby RJ. Experimental and kinetic modeling of kerosene-type fuels at gas turbine operating conditions. J Eng Gas Turb Power 2007;129:655–663.

[7] Heneghan SP, Locklear SL, Geiger DL, Anderson SD, Schulz WD. Static tests of jet fuel thermal and oxidative stability. J Prop Power 1993;9:5–9.

[8] Honnet S, Seshadri K, Niemann U, Peters N. A surrogate fuel for kerosene. Proc Comb Inst 2009;32:485–492.

[9] Huang H, Sobel DR, Spadaccini LJ. Endothermic heat sink of hydrocarbon fuels for scramjet cooling. 38th AIAA/ASME/SAE/ASEE Joint Propulsion Conference 2002; AIAA 2002-3871.

[10] Humer S, Frassoldati A, Granata A, Faravelli T, Ranzi E, Seiser R, Seshadri K. Experimental and kinetic modeling study of combustion of JP-8, its surrogates and reference components in laminar nonpremixed flows. Proc Comb Inst 2007;31:393–400.

[11] Lenhert DB, Miller DL, Cernansky NP. The oxidation of JP-8, Jet-A, and their surrogates in the low and intermediate temperature regime at elevated pressures. Comb Sci Tech 2007;179:845–861.

[12] Lindstedt RP, Maurice LQ. Detailed chemical-kinetic model for aviation fuels. J Prop Power 2000;16:187–195.

[13] Liu GZ, Han YJ, Wang L, Zhang XW, Mi ZT. Solid deposits from thermal stressing of n-dodecane and Chinese RP-3 jet fuel in the presence of several initiators. Energy Fuels 2009;23:356–365.

[14] Mawid MA, Park TW, Sekar B, Arana C. Importance of surrogate JP-8/Jet-A fuel composition in detailed chemical kinetics development. 40th AIAA/ASME/SAE/ASEE Joint Propulsion Conference 2004; AIAA 2004-4207.

[15] Mensch A, Santoro RJ, Litzinger TA, Lee SY. Shock tube study on auto-ignition characteristics of kerosene/air mixtures. Comb Flame 2010;157:1097–1105.

[16] Natelson RH, Kurman MS, Cernansky NP, Miller DL. Experimental investigation of surrogates for jet and diesel fuels. Fuel 2008;87:2339–2342.

[17] Saffaripour M, Zabeti P, Dworkin S, Zhang Q, Guo H, Liu F, Smallwood G, Thomson M. A numerical and experimental study of a laminar sooting coflow Jet-A1 diffusion flame. Proc Comb Inst 2011;33:601–608.

[18] Schulz WD. Analysis of jet fuel additives. Symposium on the Structure of Jet Fuels III, Am Chem Soc 1992:477–483.

[19] Vasu SS, Davidson DF, Hanson RK. Jet fuel ignition delay times: Shock tube experiments over wide conditions and surrogate model predictions. Comb Flame 2008;152:125–143.

[20] Violi A, Yan S, Eddings EG, Sarofim AF, Granata S, Faravelli T, Ranzi E. Experimental and kinetic modeling of kerosene-type fuels at gas turbine operating conditions. Comb Sci Tech 2002;174:399–417.

[21] Wood CP, McDonell VG, Smith RA, Samuelsen GS. Development and application of a surrogate distillate fuel. J Prop 1989;5:399–405.

[22] Zhang Y, Huang ZH, Wang JH, Xu SL. Shock tube study on auto-ignition characteristics of kerosene/air mixtures. Chinese Sci Bul 2011;56:1399–1406.

[23] Agosta A, Cernansky NP, Miller DL, Faravelli T, Ranzi E. Reference components of jet fuels: Kinetic modeling and experimental results. Exp Therm Fluid Sci 2004;28:701–708.

[24] Farmer RC, Anderson PG, Cheng GC. Propellant chemistry for CFD applications. NASA Technical Report, Document ID 19960029262, SECA Inc., Huntsville, AL; 1996.

[25] Farmer RC, Cheng GC, Anderson PG. Development of a tripropellant CFD design code. NASA Technical Report CR-207893, SECA Inc., Huntsville, AL; 1997.

[26] Huber ML, Lemmon EW, Ott LS, Bruno TJ. Preliminary surrogate mixture models for the thermophysical properties of rocket propellants RP-1 and RP-2. Energy Fuels 2009;23:3083–3088.

[27] MacDonald ME, Davidson DF, Hanson RK. Decomposition Measurements of RP-1, RP-2, JP-7, n-Dodecane, and Tetrahydroquinoline in Shock Tubes. J Prop Power 2011;27:981-989.

[28] MacDonald ME, Ren W, Davidson DF, Hanson RK. Fuel and Ethylene Measurements during n-Dodecane, Methylcyclohexane, and iso-Cetane Pyrolysis in Shock Tubes. Fuel 2012, accepted for publication.

[29] Petersen EL, Davidson DF, Rohrig M, Hanson RK. High-pressure shock-tube measurements of ignition delay times in stoichiometric H_2/O_2/Ar mixtures. In: Sturtevant B, Shepherd JE, Hornung HG, editors. Shock Waves – Proceedings of the 20th International Symposium on Shock Waves, Vol. 2, River Edge, NJ: World Scientific; 1996, p. 941-946.

[30] Petersen EL, Davidson DF, Hanson RK. Ignition delay times of ram accelerator CH_4/O_2/diluent mixtures. J Prop Power 1999;1:82-91.

[31] Huber ML, Lemmon EW, Bruno TJ. Effects of RP-1 compositional variability on thermophysical properties. Energy Fuels 2009;23:5550–5555.

[32] Herbinet O, Marquaire PM, Battin-Leclerc F, Fournet R. Thermal decomposition of n-dodecane: Experiments and kinetic modeling. J Anal App Pyrolysis 2007;78:419-429.

[33] Klingbeil AE, Jeffries JB, Davidson DF, Hanson RK. Two wavelength mid-IR diagnostic for temperature and n-dodecane concentration in an aerosol shock tube. App Phys B (Lasers Optics) 2008;93:627–638.

[34] Holman RT, Deubig M, Hayes H. Pyrolysis chromatography of lipids. I. Mass spectrometric identification of pyrolysis products of hydrocarbons. Lipids 1966;1:247–253.

[35] Pitz WJ, Naik CV, Ni Mhaolduin T, Westbrook CK, Curran HJ, Orme JP, Simmie JM. Modeling and experimental investigation of methylcyclohexane ignition in a rapid compression machine. Proc Comb Inst 2007:31:267-275.

[36] Wang H, Dames E, Sirjean B, Sheen DA, Tangko R, Violi A, Lai JYW, Egolfopoulos FN, Davidson DF, Hanson RK, Bowman CT, Law CK, Tsang W, Cernansky NP, Miller DL, Lindstedt RP. A high-temperature chemical kinetic model of n-alkane (up to n-dodecane), cyclohexane, and methyl-, ethyl-, n-propyl and n-butyl-cyclohexane oxidation at high temperatures. JetSurF version 2.0, September 19, 2010.

[37] Billingsley M, Edwards T, Shafer LM, Bruno TJ. Extent and impacts of hydrocarbon fuel compositional variability for aerospace propulsion systems. 46th AIAA/ASME/SAE/ASEE Joint Propulsion Conference 2010; AIAA 2010-6824.

[38] Orme JP, Curran HJ, Simmie JM. Experimental and Modeling Study of Methyl Cyclohexane Pyrolysis and Oxidation. J Phys Chem A 2006;110:114-131.

[39] Zeppieri S, Brezinsky K, Glassman I. Pyrolysis Studies of Methylcyclohexane and Oxidation Studies of Methylcyclohexane and Methylcyclohexane/Toluene Blends. Comb Flame 1997;108:266-286.

[40] Taylor PH, Rubey WA. Evaluation of the gas-phase thermal decomposition behavior of future jet fuels. Energy Fuels 1988;2:723–728.

[41] Brown TC, King KD. Very Low-Pressure Pyrolysis (VLPP) of Methyl- and Ethynl- Cyclopentanes and Cyclohexanes. Int J Chem Kinetics 1989;21:251-266.

[42] Kralikova U, Bajus M, Baxa J. Pyrolysis of Methylcyclohexane. Collection Czech Chem Comm 1987;52:1527-1544.

[43] Lander H, Nixon AC. Endothermic fuels for hypersonic vehicles. J Aircraft 1971;8:200–207.

[44] Granata S, Faravelli T, Ranzi E. A wide range kinetic modeling study of the pyrolysis and combustion of naphthenes. Comb Flame 2003;132:533–544.

[45] Hong Z, Lam KY, Davidson DF, Hanson RK. A comparative study of the oxidation characteristics of cyclohexane, methylcyclohexane, and n-butylcyclohexane at high temperatures. Comb Flame 2011;158:1456-1468.

[46] McEnally CS, Pfefferle LD. Fuel decomposition and hydrocarbon growth process for substituted cyclohexanes and for alkenes in nonpremixed flames. Proc Comb Inst 2005;30:1425–1432.

[47] Albright LF, Crynes BL, Corcoran WH. Pyrolysis: Theory and Industrial Practice. New York, NY: Academic Press; 1983.

[48] Frey FE, Hepp HJ. Thermal decomposition of simple paraffins. Ind Eng Chem 1933;25:441–449.

[49] Frey FE. Pyrolysis of saturated hydrocarbons. Ind Eng Chem 1934;26:198–203.

[50] Tilicheev MD. Kinetics of cracking of hydrocarbons under pressure. For Petrol Tech 1939;7:209–224.

[51] Greensfelder BS, Voge HH. Catalytic cracking of pure hydrocarbons. Ind Eng Chem 1945;37:514–520.

[52] Voge HH, Good GM. Thermal cracking of higher paraffins. J Am Chem Soc 1949;71:593–597.

[53] Zhou P, Crynes BL. Thermolytic reactions of dodecane. Ind Eng Chem Proc Des Dev 1986;25:508–514.

[54] Zhou P, Hollis OL, Crynes BL. Thermolysis of higher molecular weight straight-chain alkanes (C9-C22). Ind Eng Chem Res 1987;26:846–852.

[55] Yoon EM, Selvaraj L, Song C, Stallman JB, Coleman MM. High-temperature stabilizers for jet fuels and similar hydrocarbon mixtures. 1. Comparative studies of hydrogen donors. Energy Fuels 1996;10:806–811.

[56] Yoon EM, Selvaraj L, Eser S, Coleman MM. High-temperature stabilizers for jet fuels and similar hydrocarbon mixtures. 2. Kinetic studies. Energy Fuels 1996;10:812–815.

[57] Yu J, Eser S. Kinetics of supercritical-phase thermal decomposition of (C10-C14) normal alkanes and their mixtures. Ind Eng Chem Res 1997;36:585–591.

[58] Watanabe M, Adschiri T, Arai K. Overall rate constant of pyrolysis of n-alkanes at a low conversion level. Ind Eng Chem Res 2001;40:2027–2036.

[59] Dahm KD, Virk PS, Bounaceur R, Battin-Leclerc F, Marquaire PM, Fournet R, Daniau E, Bouchez M. Experimental and modelling investigation of the thermal decomposition of n-dodecane. J Anal App Pyrol 2004;71:865-881.

[60] Wang QD, Wang JB, Li JQ, Tan NX, Li SY. Reactive molecular dynamics simulation and chemical kinetic modeling of pyrolysis and combustion of n-dodecane. Comb Flame 2011;158:217–226.

[61] Jiang R, Liu G, You Z, Luo M, Wang X, Wang L, Zhang X. On the critical points of thermally cracked hydrocarbon fuels under high pressure. Ind Eng Chem Res 2011;50:9456–9465.

[62] Liu G, Han Y, Wang L, Zhang X, Mi Z. Supercritical thermal cracking of n-dodecane in presence of several initiative additives: Products distribution and kinetics. Energy Fuels 2008;22:3960–3969.

[63] Gascoin N, Gillard P, Bernard S, Bouchez M. Characterization of coking activity during supercritical hydrocarbon pyrolysis. Fuel Proc Tech 2008;89:9456–9465.

[64] Davidson DF, Oehlschlaeger MA, Hanson RK. Methyl concentration time-histories during iso-octane and n-heptane oxidation and pyrolysis. Proc Comb Inst 2007;31:321–328.

[65] Edwards T, Liquid Fuels and Propellants for Aerospace Propulsion, J Prop Power 2003;19:1089-1107.

[66] Westbrook CK, Pitz WJ, Herbinet O, Curran HJ, Silke EJ. A Comprehensive Detailed Chemical Kinetic Reaction Mechanism for Combustion of n-Alkane Hydrocarbons from n-Octane to n-Hexadecane. Comb Flame 2009;156:181-199.

[67] Oehlschlaeger MA, Steinberg J, Westbrook CK, Pitz WJ. The autoignition of iso-cetane at high to moderate temperatures and elevated pressures: Shock tube experiments and kinetic modeling. Comb Flame 2009;156:2165-2172.

[68] Sharpe SW, Johnson TJ, Sams RL, Chu PM, Rhoderick GC, Johnson PA. Gas-phase database for quantitative infrared spectroscopy. App Spec 2004:58:1452-1461.